

# Theoretical Investigations of a Supersonic Laminar Boundary Layer With Foreign-Gas Injection<sup>†</sup>

STEVEN I. FREEDMAN\* JOHN R. RADBILL\*\* JOSEPH KAYE‡

## Summary

The phenomena arising from the uniform injection of helium, air, argon, and iodine into the laminar boundary layer of a supersonic stream of air in a tube were investigated theoretically. The partial differential equations describing the energy, mass, and momentum transfers through the boundary layer were obtained, and a series solution was found for the case of uniform injection through the tube wall. The results of the analysis are in the form of axial distributions of wall temperature and recovery factor and of radial distribution of concentration, velocity, static, and stagnation temperatures. The gas mixture was assumed to be a perfect gas. Properties of the mixture were calculated in accordance with the Gibbs-Dalton rule and the mixing rules based on the kinetic theory of dilute gases. Transport properties for pure air were taken from the N.B.S. tabulations. Transport properties for the other gases were calculated by kinetic-theory methods, employing a Lennard-Jones 6-12 model for the interaction potential. The theoretical predictions for the recovery factor along the tube with air or argon injection agree with experimental data to within one percent. The theoretical predictions for helium injection indicate an 8-percent rise in the recovery factor along the tube, while experiments have shown only a 1-percent rise. These differences between theory and experiment are attributed to inaccuracies in the approximations to the transport properties of the binary mixtures.

## Symbols

$A$	= coefficient in series for core density
$a$	= tube radius
$B$	= coefficient in series for pressure
$c$	= mass concentration
$c_p$	= specific heat
$D$	= diffusion coefficient
$d$	= coefficient in series for $pD/T$
$f$	= coefficient in stream function series
$g$	= coefficient in concentration series
$k$	= ratio of specific heats
$M$	= Mach number
$p$	= pressure
$Pr$	= Prandtl number
$R$	= gas constant
$Re$	= Reynolds number
$r$	= radial coordinate

$Sc$	= Schmidt number
$T$	= temperature
$t$	= coefficient in temperature series
$u$	= radial velocity
$V$	= speed
$W$	= axial velocity at tube entrance
$w$	= axial velocity
$z$	= axial coordinate
$\gamma$	= coefficients in core velocity series
$\xi$	= modified Reynolds number
$\eta$	= wall distance parameter
$\theta$	= coefficient in temperature series
$\lambda$	= thermal conductivity
$\mu$	= viscosity
$\rho$	= density
$\psi$	= stream function

## Subscripts

$c$	= core quantity
$D$	= based on diameter
$I$	= injection condition
$0$	= entrance value
$w$	= wall quantity
$1,2,3$	= order of terms in series
$1,2$	= species 1 and 2
$12$	= ratio of properties of species 1 to species 2

## Introduction

RECENT DEVELOPMENTS in hypersonic flow have shown the severity of aerodynamic heating, wherein high temperatures are encountered in stagnation regions and regions of high rates of shear. Among the various methods proposed for the alleviation of these high-surface temperatures is one based on the injection of gas through the surface into the fluid. The injected gas, in addition to cooling by absorbing energy during phase changes and by being heated from a low-storage temperature to the surface temperature, affects the mechanisms of viscous dissipation and heat conduction in the boundary layer. In this paper the laminar supersonic boundary layer will be examined for the case of uniform injection of various gases. The present investigation differs from previous work because of the physical boundary condition of the uniform injection rate. The uniform injection rate case does not possess a similarity transformation, consequently the extensive results of similarity investigations are inapplicable. Theoretical solutions are presented for flow in a tube with a pressure gradient, determined by the closing of the boundary layer in the tube. This physical situation was chosen in order to have a model for comparison with experiments, which

Received by IAS April 13, 1962. Revised and received October 10, 1962.

<sup>†</sup> This research program was supported in part by the Office of Naval Research under Contract Number N5-Ori-07897, in part by the Air Research and Development Command under Contract Number AFL8(600)-1493, and in part by the M.I.T. Computation Center.

\* Assistant Professor of Mechanical Engineering, Massachusetts Institute of Technology.

\*\* Specialist—Research, Space Sciences Laboratory, North American Space and Information Systems.

‡ Late Professor of Mechanical Engineering, Massachusetts Institute of Technology.

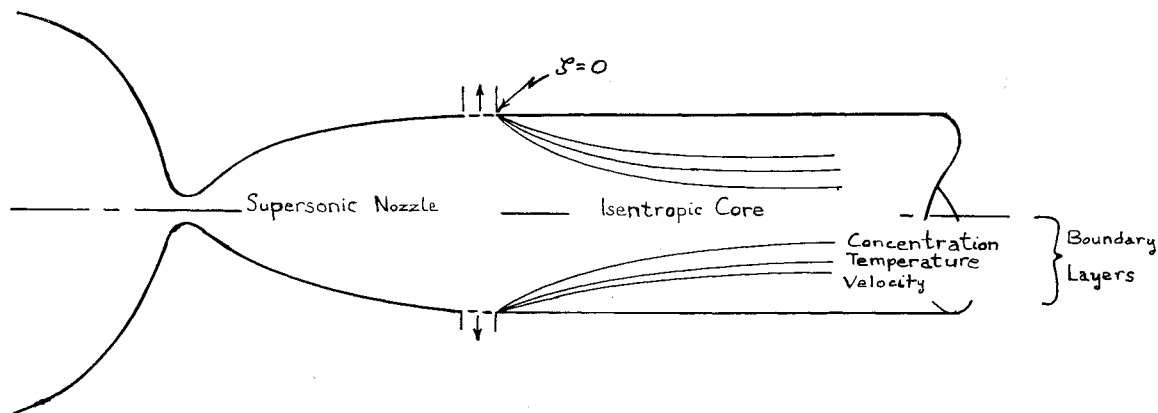


FIG. 1. Model for tube flow.

are being reported separately, by Gouse, Brown, and Kaye.<sup>1</sup>

Consider the supersonic flow of air in the entrance region of the tube shown in Fig. 1. Such a flow may be achieved by a supersonic nozzle followed by controlled boundary-layer suction. A gas is continuously injected uniformly through the porous wall into the supersonic stream.

### Assumptions

(1) The boundary-layer approximations to the Navier-Stokes equations suffice to predict the flow in the entrance region of a tube.

(2) Laminar flow exists in the boundary layer, and isentropic flow in the core.

(3) The flow is steady, axisymmetric, and with no azimuthal flow.

(4) The perfect gas and the Gibbs-Dalton rules adequately describe the thermodynamic properties.

(5) The Chapman-Enskog method of obtaining the transport properties of a dilute gas is valid.

(6) The second coefficient of viscosity is negligible.

(7) The thermal diffusion effect and other higher order coupled effects are negligible.

(8) The Prandtl and Schmidt numbers are of the order unity.

(9) Radiation within the gas is negligible.

(10) The tube is of constant cross-sectional area and of a porous, nonconducting material.

(11) The injection velocity is radial and is sufficiently large so that the air in the tube does not diffuse through the pores.

### Analysis

The desired solution describes the flow in terms of the radial and axial profiles of velocity, temperature, pressure, and concentration of foreign gas. In particular, we seek to determine the effect of gas injection on the adiabatic wall temperature as a function of the mass flux of injected gas and other pertinent variables.

The following set of boundary-layer equations, in terms of the dimensionless physical variables, have

been obtained by Radbill<sup>2</sup> by performing an order of magnitude examination of the Navier-Stokes equations expressed in cylindrical coordinates. Eqs. (1-5) describe the flow in the boundary layer in Fig. 1.

Overall continuity

$$\partial/\partial r(r\rho u) + \partial/\partial z(r\rho w) = 0 \quad (1)$$

Momentum,  $r$  direction

$$\partial p/\partial r = 0 \quad (2)$$

Momentum,  $z$  direction

$$\rho \left( u \frac{\partial w}{\partial r} + w \frac{\partial w}{\partial z} \right) = \frac{2}{Re_{D_0}} \frac{1}{r} \frac{\partial}{\partial r} \left( r\mu \frac{\partial w}{\partial r} \right) - \frac{\partial p}{\partial z} \quad (3)$$

Single-species continuity

$$\rho \left( u \frac{\partial c}{\partial r} + w \frac{\partial c}{\partial z} \right) = \frac{2}{Re_{D_0} Sc_0} \frac{1}{r} \frac{\partial}{\partial r} \left( r\rho D \frac{\partial c}{\partial r} \right) \quad (4)$$

Energy

$$\begin{aligned} c_{P2} [c(c_{P12} - 1) + 1] \rho \left( u \frac{\partial T}{\partial r} + w \frac{\partial T}{\partial z} \right) = \\ \frac{2}{Re_{D_0} Pr_0} \frac{1}{r} \frac{\partial}{\partial r} \left( r\lambda \frac{\partial T}{\partial r} \right) + \frac{2}{Re_{D_0} Sc_0} \rho D \frac{\partial c}{\partial r} \frac{\partial}{\partial r} \times \\ [Tc_{P2}(c_{P12} - 1)] + M_0^2(k - 1) w \times \\ \frac{\partial p}{\partial z} + \frac{2}{Re_{D_0}} M_0^2(k - 1)\mu \left( \frac{\partial w}{\partial r} \right)^2 \end{aligned} \quad (5)$$

Equation of state

$$p = \rho RT \quad (6)$$

Eq. (7) expresses the condition that the flow in the central part of the tube be isentropic.

$$p_c/p_0 = (\rho_c/\rho_0)^k \quad (7)$$

The solution to Eqs. (1)-(5) must satisfy the physical conditions at the wall and match the isentropic core condition.

The dimensionless variables were obtained by dividing the values of the variables by their value in the free stream at the entrance to the tube. The pressure being divided by  $(\rho W^2)_0$ , the free-stream temperature was 56.5 °K.

## Method of Solution

### Transformation to Ordinary Differential Equations

A stream function,  $\psi$ , is introduced which identically satisfies Eq. (1)

$$\rho_{ur} \equiv -\partial\psi/\partial z \quad \rho_{wr} \equiv \partial\psi/\partial r \quad (8)$$

Eq. (2) is satisfied by noting that the pressure is a function only of  $z$ . Thus a solution is needed for three differential equations: motion in the  $z$  direction, single-species continuity, and energy.

The variables in these equations were transformed from the  $(r, z)$  plane to the  $(\eta, \zeta)$  plane. Each physical variable was assumed to be given by a power series in  $\zeta$ , see Eqs. (11)–(22).

When such series are substituted into the reduced boundary-layer equations and coefficients of equal powers of  $\zeta$  are equated, then the resulting sets of ordinary differential equations may be integrated, and the unknown functions of  $\eta$  may be obtained. We choose  $\eta$  and  $\zeta$  such that the lowest order set of equations predicts that flow which is identical with the flow over a flat plate without a pressure gradient. Then the higher-order terms in the series yield corrections to this flat-plate solution; these corrections are attributed to the effects of the pressure gradient, of the injection of the gas through the porous wall, and of the curved geometry of the tube.

The  $\eta$  and  $\zeta$  are defined by

$$\eta \equiv [1 - (r/a)^2]/4\zeta \quad (9)$$

$$\zeta \equiv 2(Re_{z0})^{1/2}/Re_{D_0} \quad (10)$$

The four independent variables, reduced temperature,  $\theta$ , reduced pressure,  $p$ , concentration of injected gas,  $c$ , and stream function,  $f$ , are sufficient to determine the flow field, but introduction of additional dependent variables simplified both the derivation and the final equations used for machine computations. The following 12 series are introduced:

$$\psi = -a^2 \rho_0 W f_m(\eta) \zeta^m \quad (11)$$

$$w = w_m(\eta) \zeta^{m-1} \quad (12)$$

$$T = \theta_m(\eta) \zeta^{m-1} \quad (13)$$

$$\rho = \rho_m(\eta) \zeta^{m-1} \quad (14)$$

$$c = g_m(\eta) \zeta^{m-1} \quad (15)$$

$$p = 1 + B_m \zeta^m \quad (16)$$

$$T_c = 1 + t_m \zeta^m \quad (17)$$

$$w_c = 1 + \gamma_m \zeta^m \quad (18)$$

$$\rho_c = 1 + A_m \zeta^m \quad (19)$$

$$\mu = \mu_m(\eta) \zeta^{m-1} \quad (20)$$

$$\lambda = \lambda_m(\eta) \zeta^{m-1} \quad (21)$$

$$\rho D = d_m(\eta) \zeta^{m-1} \quad (22)$$

The equations determining the first three orders of the series solution are:

### Zero Order Momentum

$$(\mu_1 w_1')' + f_1 w_1' = 0 \quad (23a)$$

### Single-species continuity

$$\frac{1}{Sc_0} (d_1 g_1')' + f_1 g_1' = 0 \quad (23b)$$

### Energy

$$\frac{1}{Pr_0} (\lambda_1 \theta_1')' + f_1 \theta_1' + M_0^2 (k-1) \mu_1 w_1'^2 = 0 \quad (23c)$$

### First Order Momentum

$$(\mu_1 w_2' + \mu_2 w_1' - 4\eta \mu_1 w_1')' + 2f_2 w_1' + f_1 w_2' - f_1' w_2 - \frac{2B_1}{kM_0^2} = 0 \quad (24a)$$

### Single-species continuity

$$\frac{1}{Sc_0} (d_1 g_2')' + f_1 g_2' - f_1' g_2 = 0 \quad (24b)$$

### Energy

$$\begin{aligned} \frac{1}{Pr_0} (\lambda_1 \theta_2' + \lambda_2 \theta_1' - 4\eta \lambda_1 \theta_1')' + (c_{p12} - 1) g_2 f_1 \theta_1' + \\ 2f_2 \theta_1' - f_1' \theta_2 + f_1 \theta_2' + \\ \frac{d_1}{Sc_0} (c_{p12} - 1) g_2' \theta_1' + \frac{2(k-1)}{k} B_1 w_1 + \\ M_0^2 (k-1) (\mu_2 w_1'^2 + 2\mu_1 w_1 w_2' - 4\eta \mu_1 w_1'^2) = 0 \end{aligned} \quad (24c)$$

### Second Order Momentum

$$\begin{aligned} [\mu_1 w_3' + \mu_2 w_2' + \mu_3 w_1' - 4\eta (\mu_1 w_2' + \mu_2 w_1')] + \\ 3f_3 w_1' + 2f_2 w_2' + f_1 w_3' - 2w_2 f_1' - w_2 f_2' - \\ \frac{4B_2}{kM_0^2} = 0 \end{aligned} \quad (25a)$$

### Single-species continuity

$$\begin{aligned} \frac{1}{Sc_0} (d_1 g_3' + d_2 g_2' - 4\eta d_1 g_2')' + 2f_2 g_2' + \\ f_1 g_3' - f_2' g_2 - 2f_1' g_3 = 0 \end{aligned} \quad (25b)$$

### Energy

$$\begin{aligned} \frac{1}{Pr_0} [\lambda_1 \theta_3' + \lambda_2 \theta_2' + \lambda_3 \theta_1' - 4\eta (\lambda_1 \theta_2' + \lambda_2 \theta_1')] + \\ (c_{p12} - 1) [g_3 f_1 \theta_1' + g_2 (2f_2 \theta_1' + f_1 \theta_2' - f_1' \theta_2) + \\ 3f_3 \theta_1' + 2f_2 \theta_2' + f_1 \theta_3' - f_2' \theta_2 - 2f_1' \theta_3 + \\ \frac{1}{Sc_0} (c_{p12} - 1) [d_1 g_3' + g_2' (d_2 \theta_1' + d_1 \theta_2') - \\ 4\eta d_1 g_2' \theta_1'] + \frac{2(k-1)}{k} (2B_2 w_1 + B_1 w_2) + \\ M_0^2 (k-1) [2\mu_1 w_3' w_1' + \mu_1 w_2'^2 + 2\mu_2 w_1' w_2' + \\ \mu_3 w_1'^2 - 4\eta (\mu_2 w_1'^2 + 2\mu_1 w_1' w_2')] = 0 \end{aligned} \quad (25c)$$

The density is related to the temperature, pressure, and concentration by the relations

$$\rho_1 = \theta_1^{-1} \quad (26a)$$

$$\rho_2/\rho_1 = B_1 - (\theta_2/\theta_1) - g_2(M_{21} - 1) \quad (26b)$$

$$\frac{\rho_3}{\rho_1} = B_2 - \frac{\theta_3}{\theta_2} - g_3(M_{21} - 1) + \frac{\theta_2}{\theta_1} \left( \frac{\theta_3}{\theta_1} - B_1 \right) + g_2(M_{21} - 1) \frac{\rho_2}{\rho_1} \quad (26c)$$

The first derivatives,  $f_1'$ ,  $f_2'$ , and  $f_3'$ , of the stream function are related to the axial velocity and density by

$$f_1' = 2\rho_1 w_1 \quad (27a)$$

$$f_2' = 2(\rho_1 w_2 + \rho_2 w_1) \quad (27b)$$

$$f_3' = 2(\rho_1 w_3 + \rho_2 w_2 + \rho_3 w_1) \quad (27c)$$

Coefficients in the transport-property series of Eqs. (16), (21), and (22) were obtained from Taylor series expansions in  $\zeta$  with temperature and concentration as intermediate variables given as follows:

*Zero Order*

$$\mu_1 = \mu_1(\theta_1) \quad (28)$$

$$\lambda_1 = \lambda_1(\theta_1) \quad (29)$$

$$d_1 = (1/\theta_1)(pD/T)_{T=\theta_1} \quad (30)$$

*First Order*

$$\mu_2 = \left( \frac{\partial \mu}{\partial T} \right)_{T=\theta_1, c=0} \theta_2 + \left( \frac{\partial \mu}{\partial c} \right)_{T=\theta_1, c=0} g_2 \quad (31)$$

$$\lambda_2 = \left( \frac{\partial \lambda}{\partial T} \right)_{T=\theta_1, c=0} \theta_2 + \left( \frac{\partial \lambda}{\partial c} \right)_{T=\theta_1, c=0} g_2 \quad (32)$$

$$d_2 = \left[ \frac{\partial}{\partial T} \left( p \frac{D}{T} \right)_{T=\theta_1, c=0} \right] \theta_2 - \left( p \frac{D}{T} \right)_{T=\theta_1, c=0} g_2 (M_{21} - 1) \quad (33)$$

*Second Order*

$$\mu_3 = \frac{\theta_2^2}{2} \left( \frac{\partial^2 \mu}{\partial T^2} \right)_{T=\theta_1, c=0} + \theta_3 \left( \frac{\partial \mu}{\partial T} \right)_{T=\theta_1, c=0} + \frac{g_2^2}{2} \left( \frac{\partial^2 \mu}{\partial c^2} \right)_{T=\theta_1, c=0} + g_3 \left( \frac{\partial \mu}{\partial c} \right)_{T=\theta_1, c=0} \quad (34)$$

$$\lambda_3 = \frac{\theta_2^2}{2} \left( \frac{\partial^2 \lambda}{\partial T^2} \right)_{T=\theta_1, c=0} + \theta_3 \left( \frac{\partial \lambda}{\partial T} \right)_{T=\theta_1, c=0} + \frac{g_2^2}{2} \left( \frac{\partial^2 \lambda}{\partial c^2} \right)_{T=\theta_1, c=0} + g_3 \left( \frac{\partial \lambda}{\partial c} \right)_{T=\theta_1, c=0} \quad (35)$$

The coefficients in the core-property series,  $A_i$ ,  $B_i$ , and  $t_i$  are related to the core-velocity coefficient,  $\gamma_i$ , by means of the perfect-gas and isentropic flow relationships as follows:

$$p_0(1 + B_m \zeta^m) = \rho_0 R T_0 (1 + A_n \zeta^n) (1 + t_i \zeta^i) \quad (36)$$

$$1 + B_m \zeta^m = (1 + A_n \zeta^n)^k \quad (37)$$

The right-hand side of Eq. (37) is expanded by the multinomial theorem

$$1 + B_m \zeta^m = \sum_{(\sum n_i = k)} \left\{ \frac{k!}{n!} \prod_{i=1}^{\infty} (A_i \zeta^i)^{n_i} \right\} \quad (38)$$

The adiabatic condition for the isentropic core in terms of the core-property series is

$$T_c + \frac{w_c^2}{2c_p} = T_0(1 + t_m \zeta^m) + \frac{W^2}{2c_p} (1 + \gamma_n \zeta^n)^2 \quad (39)$$

Combining Eqs. (38) and (39) and equating powers of  $\zeta$  to zero yields:

$$A_1 = -M_0^2 \gamma_1 \quad (40a)$$

$$A_2 = -M_0^2 \gamma_2 + \frac{M_0^2 \gamma_1^2}{2} [(2 - k)M_0^2 - 1] \quad (40b)$$

$$A_3 = -M_0^2 \gamma_3 + M_0^2 \gamma_1 \gamma_2 [(2 - k)M_0^2 - 1] + M_0^4 \frac{\gamma_1^3 (2 - k)}{k} \left[ 1 - \frac{(3 - 2k)}{3} M_0^2 \right] \quad (40c)$$

$$B_1 = -k M_0^2 \gamma_1 \quad (41a)$$

$$B_2 = -k M_0^2 \gamma_2 + \frac{k M_0^2 \gamma_1^2}{2} (M_0^2 - 1) \quad (41b)$$

$$B_3 = -k M_0^2 \gamma_3 + k M_0^2 \gamma_1 \gamma_2 (M_0^2 - 1) + \frac{k M_0^4 \gamma_1^3}{2} \left[ 1 - \frac{(2 - k)}{3} M_0^2 \right] \quad (41c)$$

$$t_1 = -(k - 1) M_0^2 \gamma_1 \quad (42a)$$

$$t_2 = -(k - 1) M_0^2 (\gamma_2 + \gamma_1^2/2) \quad (42b)$$

$$t_3 = -(k - 1) M_0^2 (\gamma_3 + \gamma_1 \gamma_2) \quad (42c)$$

### Boundary Conditions

The boundary conditions on the ordinary differential equations [Eqs. (23)–(25)] are obtained as follows: The core-velocity coefficients,  $\gamma_i$ , are determined by evaluating the change in the mass flux along the tube. The  $\gamma_i$  become the core-boundary conditions on the boundary-layer velocity functions,  $w_j$ , which are the asymptotic values approached by the boundary-layer variables at large  $\eta$ . The core conditions on the temperature and concentration are also obtained by requiring that the core and boundary-layer series should have the same values at the edge of the boundary layer. Thus for large values of  $\eta$ :

$$w_i = \begin{cases} 1 & i = 1 \\ \gamma_{i-1} & i \geq 2 \end{cases} \quad (43)$$

$$\theta_i = \begin{cases} 1 & i = 1 \\ t_{i-1} & i \geq 2 \end{cases} \quad (44)$$

$$g_i = 0 \quad (45)$$

The asymptotic values of  $\gamma_i$  are computed at large values of  $\eta$  and are given by:

$$\gamma_1 = 2(f_{1\infty} - 2\eta_{\infty})/(M_0^2 - 1) \quad (46a)$$

$$\gamma_2 = \gamma_1 \{ 4\eta_{\infty} - M_0^2 \gamma_1 [(2 - k)M_0^2 - 3]/2(1 - M_0^2) \} - 2f_{2\infty}/(1 - M_0^2) \quad (46b)$$

$$\gamma_3 = \left\{ M_0^2 \gamma_1^3 [(2k-3)(2-k)M_0^4/6 + (2-k)M_0^2 - 1/2] + M_0^2 \gamma_1 \gamma_2 [(2-k)M_0^2 - 3] + 2f_{3\infty} - 4\eta_\infty [M_0^2 \gamma_1 [(2-k)M_0^2 - 3]/2 + \gamma_2(1-M_0^2)] \right\} / (M_0^2 - 1) \quad (46c)$$

The boundary conditions on the velocity and stream function obtained from the zero slip condition at the wall and from the known uniform injection rate are:

$$w_i = 0 \quad (47)$$

$$f_m = \begin{cases} Re_{DI}/2 & m = 2 \\ 0 & m \neq 2 \end{cases} \quad (48)$$

where

$$Re_{DI} \equiv Re_{D0}[(\rho u)_{wall}/(\rho_0 W)] \quad (49)$$

The boundary conditions for the single-species continuity equations are given by Eqs. (50a)–(50c) in terms of the mass flux of injected gas at the wall. The mass velocity at the surface,  $(\rho u)_{wall}$  can be prescribed.

$$g_1' = 0 \quad (50a)$$

$$g_2' = Sc_0 Re_{DI}/d_1 \quad (50b)$$

$$g_3' = (-1/d_1)(d_2 g_2' + g_2 Sc_0 Re_{DI}) \quad (50c)$$

The boundary condition for the energy equations [(Eqs. (23c), (24c), and (25c)] assuming an adiabatic wall, is that the temperature gradient at the wall is zero:

$$\theta_i' = 0 \quad (51)$$

### Approximations Used for the Evaluation of the Properties

The specific heats of the components of the binary mixture vary by less than 1 percent from its value at 300°K over the temperature range found in our problem. The specific heats of the binary mixtures were therefore expressed as functions of concentration only, according to the Gibbs-Dalton law.

Evaluation of transport properties for gas mixtures presented a much more difficult problem, since little data exist on the transport properties of binary mixtures; therefore the authors relied on predictions of transport properties from kinetic theory. The first approximations to transport properties of binary mixtures derived from kinetic theory are complex expressions. Kinetic theory shows that the dimensionless viscosity and thermal conductivity of a pure substance have approximately the same variation with temperature, when the specific heat does not vary much with temperature. The dimensionless viscosity was taken to be a product of a quadratic function of the reduced temperature and a separate quadratic function of the mass concentration. The dimensionless thermal conductivity was likewise taken to be a product of the same quadratic function of the reduced temperature and of a different quadratic function of the mass concentration. Since low-mass concentrations of the foreign gas were expected throughout most of the boundary layer in this study, the approximations used herein were designed to fit the temperature variation of viscosity for pure air as closely as possible.

The expression  $pD/T$  was approximated by a quadratic function of the reduced temperature. Comparison of the more exact, but more complex, approximations to the transport properties with our quadratic function and products of quadratic functions are shown for a helium-air mixture in Fig. 2.

### Vanishing of the Zero-Order Concentration Function

In this section, the zero-order concentration function  $g_1$  will be shown to be zero throughout the boundary layer for a boundary layer with uniform injection. Physical reasoning indicates that a constant term in the concentration series means a finite concentration of foreign gas in the boundary layer at the initial injection point, where there is no doubt that foreign gas has not been previously injected. Mathematically, to show

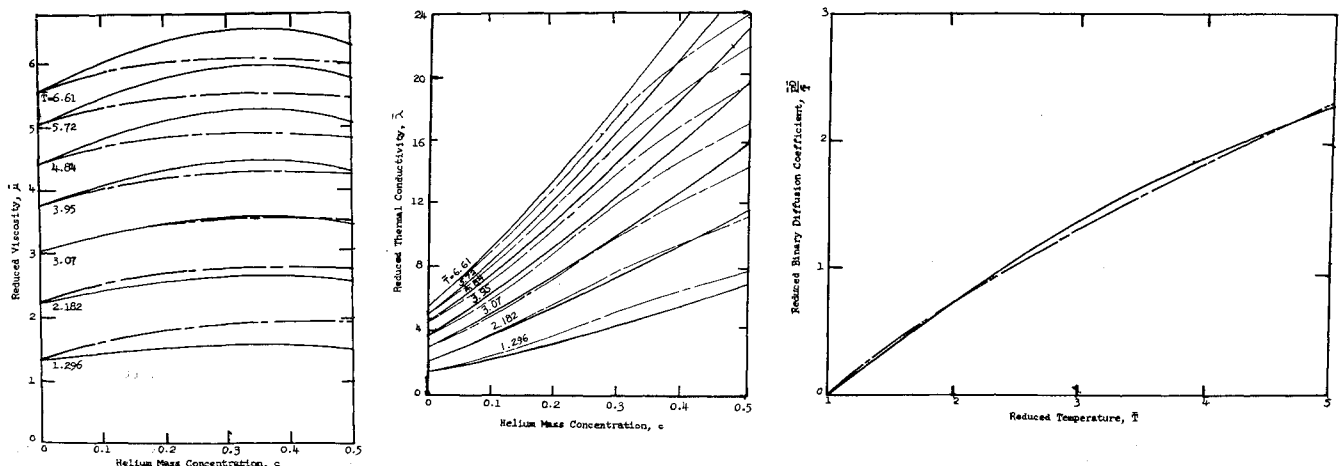


FIG. 2. Comparison of the kinetic theory calculations and the numerical approximations to the values of the transport properties.  
 ————— numerical approximation used in computations  
 - - - - - calculated from kinetic theory

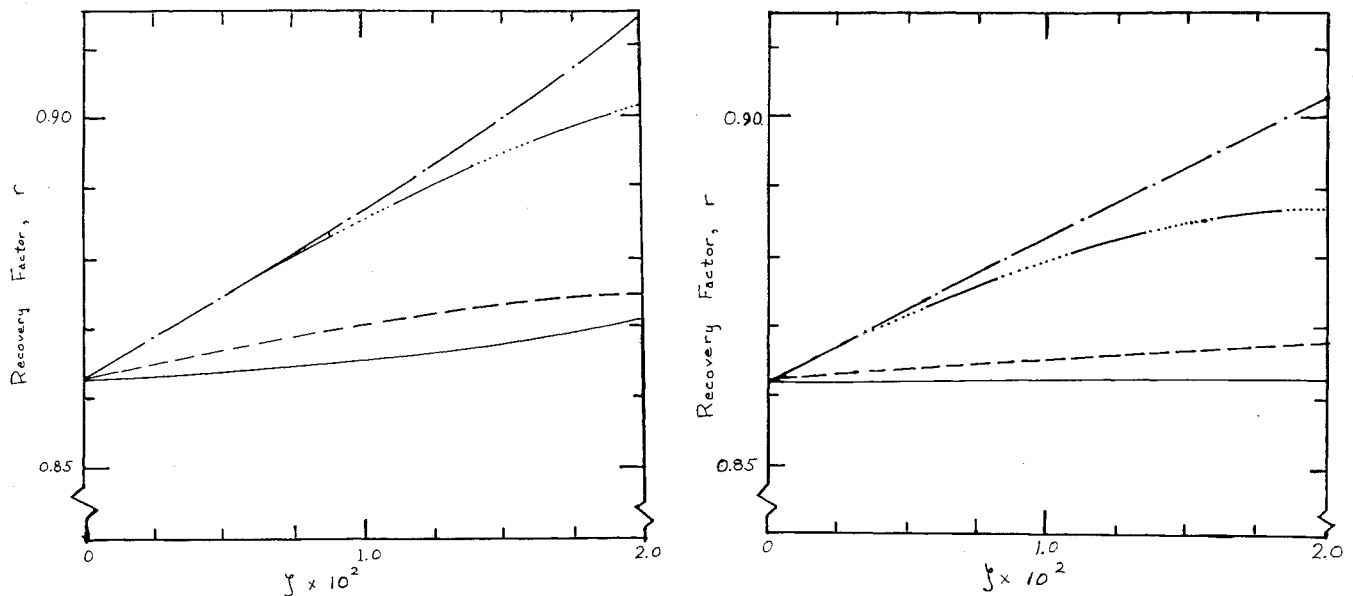


FIG. 3. Variation in recovery factor as a function of modified length Reynolds number,  $\zeta$ , for flow over a flat plate and in a tube, with and without uniform injection of helium. Pressure gradient determined for supersonic flow in a tube.

—	without pressure gradient	} $Re_{DI} = -8$
·····	with pressure gradient	
- - -	without pressure gradient	} $Re_{DI} = 0$
- · - · -	with pressure gradient	

that the constant term vanishes for the case of uniform injection, we substitute the series expressions [Eqs. (11)–(22)] into the single-species continuity equation to obtain:

$$d_m g' n \zeta^{m+n-2} = \zeta S c_0 (1 - g_1 \zeta^{l-1}) Re_{DI} \quad (52)$$

The zero-order single-species continuity equation is obtained by equating the coefficient of  $\zeta^0$  to zero

$$S c_0 g_1' + (d_1 g_1')' = 0 \quad (53)$$

The boundary condition at the wall on the zero-order single-species continuity equation has been shown to be (52)  $g_1' = 0$ . Thus the boundary conditions are

$$\eta = 0 \quad g_1' = 0 \quad \eta \rightarrow \infty \quad g_1 \rightarrow 0 \quad (54)$$

If we carry out a step-by-step integration launched from  $\eta = 0$ , we see that the value of  $g_1'$  will be zero at any point if the value of  $(d_1 g_1')'$  is zero at the preceding point, since  $d_1$  is finite and  $(d_1 g_1')'$  is zero at any point where  $g_1'$  is zero. Thus, since  $g_1'$  is zero at the initial point,  $g_1$  must have a constant value; and reference to the asymptotic boundary condition shows that this value must be zero. Hence, we need not consider the zero-order, single-species continuity equation or the function  $g_1$  and its derivatives.

### Method of Solution of the Ordinary Differential Equations

The ordinary differential equations [Eqs. (23)–(25)] were integrated one order at a time starting with the zero-order equations. Each order uses the solutions of all preceding orders as coefficients in the ordinary differential equations. The boundary conditions for every order except the zero order are also determined

by the solutions of the preceding orders. The zero-order equations are nonlinear, but all succeeding orders are linear. The complexity of even the zero-order equations was so great that a closed form analytical solution was not considered. A numerical method was employed to integrate the ordinary differential equations. A difficult feature of this integration method arose from the form of the boundary conditions which were specified both at an initial point and asymptotically at large values of the independent variable. The method finally selected was that of numerical integration.

An iterative scheme was used to find the unknown wall boundary conditions. The values of  $w_i$ ,  $\theta_j$ , and  $g_k$  were chosen at  $\eta$  equal to zero in order to start the integration. In general, the values obtained for  $w_i$ ,  $\theta_j$ , and  $g_k$  at large  $\eta$  did not match the core boundary conditions for any particular set of wall conditions. An iterative method of interpolation based on several integrations was used to converge on the correct wall and correct core boundary conditions.

### Form of Solution

The series form of solution to the boundary-layer equations consists of a major term, namely, the zero order, plus a series of higher order correction terms. The zero-order solution describes the boundary-layer flow over a flat plate without a pressure gradient and without injection. The sum of the higher-order terms describes the total changes in the boundary-layer flow caused by the tube geometry, pressure gradient, and the injection rate. Rapid convergence of the solution with respect to higher-order terms justified terminating the series-type solution with the second-order term.

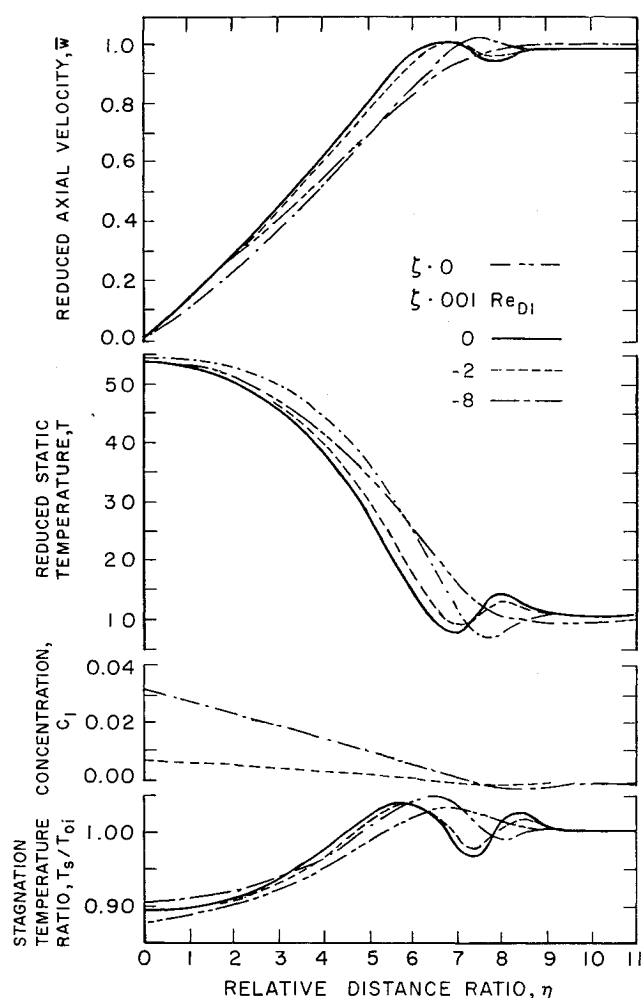


FIG. 4. Profiles of reduced axial velocity, reduced static temperature, helium mass concentration, and stagnation temperature ratio.

The zero-order  $z$ -direction momentum equation and the zero-order energy equation are independent of the injection rate and of the properties of the injected gas since the zero-order concentration function vanishes, as shown above. The solution for tube flow with a pressure gradient but without injection shows that the perturbations caused by the curvature of the tube wall and by the pressure gradient result in small changes in the velocity and temperature profiles within the limits of validity of the solution, see Fig. 3. The first- and higher-order equations, containing the effects of the injection of gas are all linear; therefore, the method of superposition of solutions can be used, and only one solution without injection and one with injection are necessary in order to obtain solutions for all injection rates.

### Region of Validity of Solutions

The profiles shown in Fig. 4 are at axial locations of  $\zeta = 0$ , and  $\zeta = 10^{-2}$ . The solution at  $\zeta = 0$  is identical with the Blasius solution with temperature dependent properties. The solution at  $\zeta = 10^{-2}$  shows why this

value of  $\zeta$  was chosen as the limit of validity of the solution. At this value of  $\zeta$ , the third term in the series solution amounts to about 8 percent of the total for typical values in the boundary layer. The contribution of the third term in the series solution to the values of the variables at the wall however are of the magnitude of 1 percent at locations where  $\zeta$  is as large as  $10^{-2}$ . The parameters of main concern in this investigation are the wall values, shear stress, diffusion flux, and temperature gradient. The series solution was terminated with the third term and therefore the region of validity was restricted to values of  $\zeta$  that are less than  $10^{-2}$ . At values of  $\zeta$  of  $10^{-2}$  the profiles show various wiggles at the edge of the boundary layer. These wiggles do not physically exist, they are manifestations of the attempt to obtain a series solution for a function in a region where it has a small radius of curvature. In this region of large curvature, the terms in the series solution alternate sign. When a small number of terms are used in the series solution irregularities of the order of the last term in the series are to be expected. This is the reason why the profiles show bumps which do not exist physically. The stagnation temperature shows the most irregularities because the stagnation temperature is computed from other series. The general trend in the stagnation temperature shows a real bump at the edge of the boundary layer attributable to the excess of kinetic and thermal energy at that location due to the difference between the conduction and dissipation rates.

The boundary-layer equations are valid only where the flow remains attached to the wall; this condition places an upper limit on the injection parameter such that the flow neither separates nor becomes turbulent. Experiments by Gouse<sup>3</sup> and by Sziklas and Banas<sup>4</sup> have shown that the largest injection parameter permissible for tube flow and cone flow corresponds to an injection Reynolds number of about  $-20$ . The minus sign on injection Reynolds number signifies that the velocity of the injected gas at the wall is away from the wall. Negative injection parameters correspond to injection while positive ones correspond to suction.

## Results

### General

Solutions to the boundary-layer equations for laminar supersonic flow of air in a tube with uniform injection of gas were obtained with the use of the IBM 704 computer at the Massachusetts Institute of Technology Computation Center for the following cases: (a) zero injection, (b) helium injection, (c) air injection, (d) argon injection, (e) iodine injection, and (f) suction.

For each case, the numerical computations resulted in profiles of temperature, pressure, concentration of injected gas, and velocities in the axial and radial directions. Recovery factor, pressure ratio, and other parameters were computed as functions of the modified length Reynolds number,  $\zeta$ , and the wall-distance

parameter  $\eta$ . All solutions presented are for an inlet Mach number of 5 and a stagnation temperature of 338.7 K (150 F). Due to space limitations, only the more interesting results are presented here. For further details, see Radbill.<sup>2</sup> The effects of the pressure gradient and of the tube geometry, for zero injection, show small changes from the zero-order solution. The effects of the uniform injection on the velocity and temperature profiles are likewise small, see Fig. 4.

### Results for Helium Injection

The concentration, velocity, static- and stagnation-temperature profiles for the case of uniform helium injection are shown in Fig. 4. These profiles are at two sections along the tube; namely, at the inlet section where the modified length Reynolds number,  $\zeta$ , is zero, and at a section downstream at a value of  $\zeta$  equal to 0.01.

Fig. 5 shows the concentration of helium at the wall as a function of the modified length Reynolds number for various injection parameters,  $Re_{DI}$ . Since the modified length Reynolds number is proportional to the square root of the distance from the tube inlet and the curves in Fig. 5 are almost straight lines, we can conclude that the concentration of helium at the wall is very nearly proportional to the square root of the distance from the tube inlet. This chart shows the manner in which the foreign gas concentration builds up along the tube wall with uniform injection.

Fig. 6 shows that uniform helium injection results in a small increase in the recovery factor along the tube. Note that an increase in the recovery factor along the tube occurs with zero injection and is attributed to the pressure gradient which exists in the tube and the closing of the boundary layer on the isentropic core. The predictions shown in Fig. 6 agree qualitatively with experimental values found by Gouse<sup>3</sup> for uniform injection. The present analysis predicts that the recovery factor should increase from 0.86 to 0.90, a 4 percent increase, at the end of the test section used in

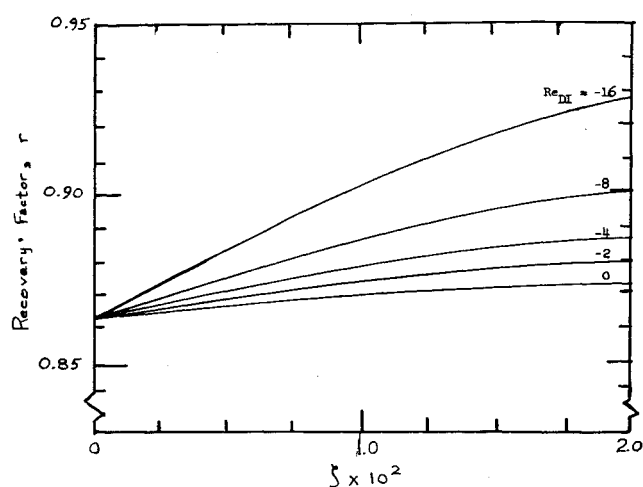


FIG. 6. Recovery factors for flow in a tube with uniform injection of helium. Pressure gradient determined by the flow.

Gouse's experiments; however, Gouse has found only a 1 percent increase in the recovery factor at the end of his test section. Experiments by Leadon and Scott<sup>5</sup> for a different geometry and a different injection method, have shown an initial increase of about 10 percent in the recovery factor for small rates of helium injection followed by a decrease in recovery factor of the same amount for larger injection rates. Although Leadon and Scott's experiments were conducted with a different injection method and for a different geometry, their recovery factor measurements exhibit the same directional trends as the present predictions.

The approximations used to obtain the transport properties of the helium-air mixture are the most probable explanation of the 5 percent difference between the uniform injection theory for helium and the experiments. Solutions to the laminar compressible boundary-layer equations are sensitive to the values of the transport properties. The effect of uncertainty in the approximations used to calculate the transport properties was studied by obtaining additional analytical solutions. These solutions employed arbitrary variations in the values of the thermal conductivity and viscosity of the helium-air mixture. The viscosity and thermal conductivity of the helium-air mixture were varied by 5 percent at a helium concentration of 0.20. There was no arbitrary change made in either the approximation to the diffusion coefficient or the viscosity and thermal conductivity of the pure air since the values used to approximate these properties agreed excellently with experimental data. These arbitrary variations were accomplished by changing the coefficients in the quadratic functions which expressed the dependence of the transport properties in the concentration of helium, see Fig. 7.

A decrease in the viscosity made by the above kind of variation of the concentration dependence of the viscosity of the helium-air mixture resulted in a decrease of the recovery factor by about 1.5 percent at a  $\zeta$  of 0.02 and for an injection rate corresponding to a value of  $Re_{DI} = -8$ . An increase in the thermal

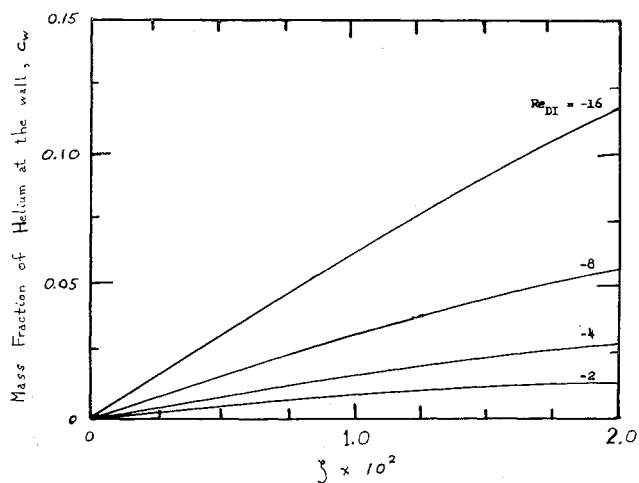


FIG. 5. Wall concentration of helium for uniform injection.



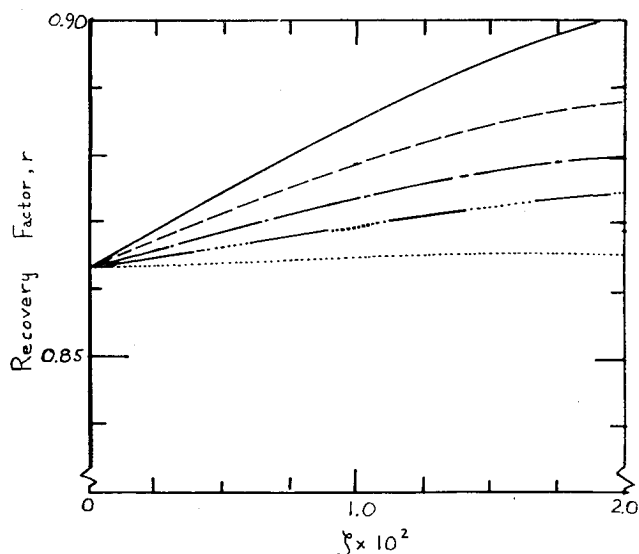


FIG. 7. Variation of recovery factor along the tube for various modifications of the approximations to the transport properties of the binary mixture,  $Re_{DI} = -8$ .

- original values
- - - modified viscosity
- · - modified thermal conductivity
- no injection reference
- - - - - modified viscosity and thermal conductivity

conductivity, in the same manner, resulted in a decrease in the recovery factor by 2 percent at a  $\xi$  of 0.02 and for an injection Reynolds number of  $-8$ . The combined effects of both of these variations in properties resulted in a 4 percent decrease in the recovery factor at the same location for the same injection rate. It is apparent that accurate predictions of the adiabatic wall temperature in a compressible laminar boundary layer of a multicomponent fluid requires accurate detailed knowledge of the temperature and concentration dependence of the transport properties of the mixture.

#### Discussion of Results for Helium Injection

The reason why helium was studied is that a helium-air mixture has transport properties which appear to be favorable for the alleviation of the high-surface temperatures encountered in aerodynamic heating. Previously Eckert, Schneider, Hayday and Larson<sup>6</sup> and Baron<sup>7</sup> have claimed that, on the basis of similarity solutions, if the rate of injection is proportional to  $z^{-1/2}$  and if the boundary-layer approximations to the Navier-Stokes equations are valid with the accompanying infinite injection velocity at the leading edge, then such injection of helium should result in a large lowering of the adiabatic wall temperature. To attain such a lowering of the adiabatic wall temperature, the fluid in the region near the wall must have a Prandtl number which is substantially lower than that of either pure air (0.71) or pure helium (0.69). Calculations by Gouse<sup>3</sup> and by Sziklas<sup>8</sup> and experiments by Eckert, Ibele, and Irvine<sup>9</sup> have shown that the Prandtl number of a helium-air mixture goes through a minimum of 0.46 at a mass concentration of about one quarter.

Analytical and experimental investigations have shown that the recovery factor in a laminar boundary layer without mass transfer is very nearly equal to the square root of the Prandtl number. The Prandtl number is characteristic of the ratio of the effects of viscous dissipation to heat conduction. The greater the Prandtl number, the larger is the ratio of viscous dissipation to heat conduction, and hence the greater the adiabatic wall temperature. We should therefore expect that in a boundary layer with mass transfer when there is a low Prandtl number, the recovery factor would be lower than for a pure air boundary layer. This is what the similarity analyses of Eckert, Schneider, Hayday, and Larson<sup>6</sup> and Baron<sup>7</sup> show. However, experiments by Gouse,<sup>3</sup> Scott, Anderson, and Elgin,<sup>10</sup> and Gouse, Brown, and Kaye,<sup>1</sup> have failed to find this large lowering of the adiabatic wall temperature.

The present analysis has found that when helium is uniformly injected into a laminar boundary layer, the recovery factor initially increases, and after a sufficient amount of helium has been injected, later decreases. The eventual decrease in the recovery factor occurs when there is enough helium in the boundary layer to lower the Prandtl number of the mixture over a significant portion of the boundary layer. The initial increase in the recovery factor which accompanies the injection of helium is attributed to the high specific heat of helium.

In order to maintain the boundary condition of zero heat flux through the wall at every section along the tube, we must inject the transpiration gas into the boundary layer at the local recovery temperature. As the injected gas diffuses away from the wall, it is accelerated by the shear stresses present in the boundary layer. Since the difference between the stagnation and static temperatures is  $V^2/2gc_p$ , helium, because of its larger  $c_p$  will experience a smaller drop in temperature when it diffuses away from the wall than would an equal mass of air, assuming adiabatic acceleration. The injection of a gas with a high specific heat into a boundary layer, composed of a gas with a low specific heat, results in the raising of the temperature of the gas mixture at locations in the boundary layer where there is a substantial amount of the injected gas. The various stream tubes in a boundary layer, however, are not in adiabatic flow, but as the Prandtl number is of the order of unity, we know that the effects of viscous dissipation and heat conduction are of the same order of magnitude. As long as we neglect the differences between the rates of viscous dissipation and heat conduction in the binary gas boundary layer as compared with a single-component boundary layer, we see that injection of a gas with a specific heat higher than that of the gas in the boundary layer results in a higher temperature in the region where there is an appreciable amount of the injected gas, as compared with zero mass transfer conditions. As a result of this diffusion, acceleration, and mixing process, we find a higher

average temperature profile across the boundary layer downstream of an injection station where a gas with a specific heat, which is larger than that of the free-stream gas, has been injected. This increase in average temperature must also result in an increase in the adiabatic wall temperature downstream from the injection location. Thus we see that if the sole effect on the gas in the boundary layer caused by the injection of gas was due to the specific heat of the injected gas, then injection of helium would result in an increased recovery factor.

The purpose of this explanation has been to describe how injection of a light-weight gas could increase the adiabatic wall temperature. The numerical solutions to the boundary-layer equations for uniform injection of helium show such an increase in the adiabatic wall temperature.

The series which was used to evaluate the adiabatic wall temperature consists of three terms. This series is a quadratic function of the modified length Reynolds number,  $\zeta$ . The constant term is the zero-order solution. The first-order coefficient in the series is positive, and the second-order coefficient is negative for the case of helium injection, showing that an effect of helium injection is to initially increase the adiabatic wall temperature and later to reverse this trend. At the initiation of injection, the effect of the high specific heat dominates. When there is enough helium in the boundary layer to alter the transport properties, then the effects of the lower Prandtl number of the gas mixture and the reduced velocity gradient become more important, and the adiabatic wall temperature thereafter decreases. Solutions were therefore calculated for gases of lower specific heats (argon and iodine).

### Results for Other Gases

Solutions to the boundary-layer equations for the uniform injection of a gas into a supersonic stream in a tube were obtained for the cases of air, argon, iodine, and for suction. The results are shown in Fig. 8 for the case of  $Re_{DI} = -8$ . These solutions are only the sum of the first two terms of the series solution as the second-order perturbation terms in the helium solution amount to small changes in the physical results in the region of validity. In order to be able to separate the effects of changing the properties of the fluid in the boundary layer from the effect of the general thickening of the boundary layer by the injected gas, solutions for air injection and suction were computed.

The suction solution shown in Fig. 8 shows an increase in recovery factor. This increase reflects the fact that suction causes a thinning of the boundary layer and an increase in the velocity gradient which results in an increased rate of viscous dissipation. Conversely, the air-injection solution thickens the boundary layer, reducing the velocity gradient and decreasing the rate of viscous dissipation. In both of these cases there are no effects caused by variations in thermodynamic (specific heat) or transport (viscosity and

thermal conductivity) properties of the gas in the boundary layer. The velocity, temperature, and concentration profiles across and along the tube show the same type of changes with helium injection as with injection of the other gases.

Inasmuch as the analytical results for air and for argon injection showed excellent agreement with experimental results, an attempt was made to find a more desirable substance for injection. The high molecular weight of iodine implies a low specific heat. Iodine also has a comparatively small size for its large molecular weight, indicating as favorable transport properties as could be expected for a molecule of this weight. A solution for iodine injection was computed, and Fig. 8 shows the extent to which reductions in the recovery factor are predicted. The relative importance of the specific heat can be clearly seen.

The computed results for argon and iodine both show a decrease in the recovery factor with injection. The specific heat of argon is about one-half that of air, and its molecular size is about 5 percent smaller than that of a typical air molecule. Inasmuch as the molecular weight is one-third greater than that of air, we can see that the viscosity and thermal conductivity of argon will not be favorable for the reduction of aerodynamic heating. However, argon has a low specific heat. The resulting recovery factor for argon injection shows a lowering of the adiabatic wall temperature. This lowering of the recovery factor is small (about 1 percent at the limits of validity of the analysis), but has been found experimentally by Gouse<sup>3</sup> and Gouse, Brown, and Kaye.<sup>1</sup> Gouse's experiments showed that helium injection increases the recovery factor, that air injection (nitrogen was used experimentally) lowers

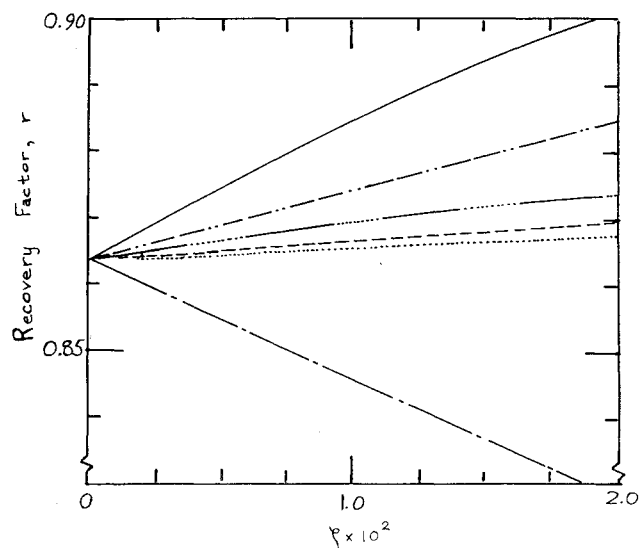


Fig. 8. Variation in recovery along the tube for injection of various gases,  $Re_{DI} = -8$ , and suction  $Re_{DI} = +8$ .

— helium injection  
 - - - suction ( $Re_{DI} = +8$ )  
 ..... no injection reference  
 - · - air injection  
 ..... argon injection  
 - · · iodine injection

the recovery factor, (1/4 percent), and that argon injection lowers the recovery factor further, (1/2 percent).

The results of this study have shown how slight variations in the dependence of the transport properties of the gas in a high-speed binary boundary layer can affect the recovery factor. Recent work by Tewfik and Eckert<sup>12</sup> and Baron<sup>13</sup> have shown that the omission of the thermal diffusion term in the diffusion and energy equations can result in incorrect recovery factors for boundary layers with mass transfer. The work of Tewfik and Eckert, and Baron supports one of the conclusions of this work, that seemingly second-order effects must be included in order to obtain accurate results. The recovery factor is very sensitive to the variations of the transport properties with the gas concentration. Precise values of the transport properties, including the thermal diffusion coefficient, are required for an accurate computation of boundary-layer transfer rates. Inclusion of the thermal diffusion terms with approximate values of transport properties for studies beyond those of Tewfik and Eckert<sup>12</sup> and Baron<sup>13</sup> seems unwarranted.

### Conclusions

A method has been developed for computing the effects of the uniform injection of foreign gas into the laminar boundary layer of a compressible gas. The method has been applied to the injection of various gases into the boundary layer which is found in a uniform tube in which there is a supersonic flow of air. Results have been obtained for the injection of helium, air, argon, and iodine vapor. These results show a general trend which indicates that uniform injection of helium will initially increase the recovery factor and will, when continued to be injected uniformly, subsequently reduce the recovery factor. Air injection lowers the recovery factor slightly as does argon (slightly more). A marked decrease in the recovery factor is found in the case of the uniform injection of iodine vapor. The helium, air, and argon results explain the experimental results of Gouse, Brown, and Kaye,<sup>1</sup> which cannot be explained in terms of the analytical results of the similarity theory.<sup>11</sup> Compari-

son with the results of similarity theory indicate similar directional trends for the variations with molecular weight.

### References

- <sup>1</sup> Gouse, S. W., Jr., Brown, G. A., and Kaye, J., *Some Effects of Injection of Foreign Gases in a Decelerating Laminar Boundary Layer in Supersonic Flow*, Journal of the Aerospace Sciences, Vol. 29, No. 10, Oct. 1962.
- <sup>2</sup> Radbill, J. R., *Analytical Investigation of the Effects of a Diffusion Field on a Laminar Boundary Layer in Supersonic Flow*, Sc.D. Thesis, Mech. Engineering Dept., M.I.T., Jan. 1958.
- <sup>3</sup> Gouse, S. W., Jr., *Experimental Investigation of the Effects of a Diffusion Field on a Laminar Boundary Layer in Supersonic Flow*, Sc.D. Thesis, Mech. Engineering Dept., M.I.T., Nov. 1957.
- <sup>4</sup> Sziklas, E. A., and Banas, C. M., *Mass Transfer Cooling in Compressible Laminar Flow, in A Symposium on Mass-Transfer Cooling for Hypersonic Flight*, sponsored by RAND and AFOSR, June 1957.
- <sup>5</sup> Leadon, B. M., and Scott, C. J., *Measurement of Recovery Factors and Heat Transfer Coefficients with Transpiration Cooling in a Turbulent Boundary Layer at  $M = 3$  Using Air and Helium as Coolants*, Univ. of Minnesota, Institute of Technology, Dept. of Aeronautical Engineering, Research Rep. No. 126, 1959.
- <sup>6</sup> Eckert, E. R. G., Schneider, P. J., Hayday, A. A., and Larson, R. M., *Mass Transfer Cooling of a Laminar Boundary Layer by Injection of a Light-Weight Foreign Gas*, Tech. Note 14, Heat Transfer Lab., Mechanical Engineering Dept., Univ. of Minnesota, June 1957.
- <sup>7</sup> Baron, J. R., *The Binary-Mixture Boundary Layer Associated with Mass Transfer Cooling at High Speeds*, M.I.T., Naval Supersonic Lab., Tech. Rep. 160, May 1956.
- <sup>8</sup> Sziklas, E. A., *An Analysis of the Compressible Laminar Boundary Layer with Foreign Gas Injection*, Rep. SR-0539-8, Research Dept., United Aircraft Corp., May 1956.
- <sup>9</sup> Eckert, E. R. G., Ibele, W. E., and Irvine, T. F., Jr., *Thermal Conductivity of Helium-Air Mixtures, Thermodynamic and Transport Properties of Gases, Liquids and Solids*, pp. 295-300, ASME and McGraw-Hill Book Co., Inc., New York, 1959.
- <sup>10</sup> Scott, C. J., Anderson, G. E., and Elgin, D. R., *Laminar, Transitional and Turbulent Mass Transfer Cooling Experiments at Mach Numbers from 3 to 5*, Research Rep. No. 162, Univ. of Minnesota, Institute of Technology, Aeronautical Engineering Dept., Aug. 1959.
- <sup>11</sup> Gross, J. F., Hartnett, J. P., Masson, D. J., and Gzeley, C., Jr., *A Review of Binary Laminar Boundary Layer Characteristics*, Int. J. Heat & Mass Transfer, Vol. 3, pp. 198-221, 1961.
- <sup>12</sup> Tewfik, O. E., and Shirliffe, C. J., *On the Coupling Between Heat and Mass Transfer*, Journal of the Aerospace Sciences, Vol. 29, No. 8, Aug. 1962.
- <sup>13</sup> Baron, J. R., *Thermodynamic Coupling in Boundary Layers* A.R.S. Journal, Vol. 32, No. 1, p. 1053, Jan. 1962.